available at www.sciencedirect.com

ScienceDirect

journal homepage: www.elsevier.com/locate/carbon

Real time monitoring of the drug release of rhodamine B on graphene oxide

Renyun Zhang [a,*], *Magnus Hummelgård* [a], *Gang Lv* [b], *Håkan Olin* [a]

[a] *Department of Natural Sciences, Engineering and Mathematics, Mid Sweden University, SE 851 70 Sundsvall, Sweden*
[b] *Department of Mathematic & Physics, North China Electric Power University, Baoding 071003, China*

ARTICLE INFO

Article history:
Received 5 July 2010
Accepted 14 November 2010
Available online 18 November 2010

ABSTRACT

A real time method for monitoring the drug load and release on graphene oxide (GO) in a cuvette is reported using rhodamine B (RB) as a model for a drug. The mechanisms of the release of RB at different pH were investigated, by monitoring the time dependency of the accumulative drug release. In vitro real time experimental results indicated that RB could be loaded on GO with a capacity of 0.5 mg/mg. The drug release of RB was pH sensitive as observed at pH 7.4 and pH 4.5 PBS solutions. The higher pH values lead to weaker hydrophobic force and hydrogen bonds, and thus higher release rate. The ionic strength also influenced the release of RB, as shown from the different release rates between PBS solutions and double distilled water. These results indicated a case II transport process at pH 7.4 and an anomalous diffusion process at pH 4.5 and in water. The method described here allows real time detection of the drug release rate, in contrast to common dialysis analysis. This method also points to other real time detections in biomedical investigations.

1. Introduction

Multifunctional nanomaterials with functional surface groups or structures that can be used to load drug molecules, or nanostructures that can be used to assist the drug delivery are desired in biomedical research [1–5]. New opportunities to improve the cure efficiency are being made available due to the nanostructural properties as mentioned above, for example, new technologies allow the creation of materials that are small enough to interact with target biological molecules through the derivation of the surface structure [3]. Nanotechnology, as one of these new technologies, allows the fabrication of nanoscaled devices that can combine device technology with therapeutic molecules to create implantable devices or to do in vivo therapeutic treatment [6].

Nanoparticles like Au [7], Fe_3O_4 [4], and polymers [8–10] have already been used in several areas of drug delivery, with particle size less than 100 nm. Drug molecules can be linked to the nanoparticles through hydrophobic force [4], electrostatic interaction [11], or the drugs can be conjugated with polymer nanoparticles [6]. Recently, several reports on drug delivery have focused on the new 2D nanomaterial, graphene oxide [12–15], showing ultra-high drug loading capacity. The two sides of graphene oxide sheet can be accessible for drug binding, which contributes to the high drug-loading amount.

The loading capacity of doxorubicin (DXR) on graphene oxide is up to 2.35 mg/mg [14], while it is usually below 1 mg/mg for other nanomaterials [14]. Moreover, the graphitic nanocarriers like graphene oxide can afford strong noncovalent binding with aromatic drugs through simple adsorption [12], and it can be used to carry some insoluble drugs [12], which is desired in future device fabrication since many drugs are not water soluble [6].

Drug load and release experiments in buffer and living cells have been done in the above-mentioned reports, mostly work with DXR, and empirical interaction between DXR and

* *Corresponding author:* Fax: +46 60 148802.
E-mail address: renyun.zhang@miun.se (R.Y. Zhang).
0008-6223/$ - see front matter
doi:10.1016/j.carbon.2010.11.026

graphene oxide is suggested. However, there is no report on the real time detection of drug load and release of molecules on graphene oxide. Also, studies on the mechanism of the drug release from GO at different pH and solvent is lacking.

Here, we describe a new method for real time monitoring of drug load and release on GO using rhodamine B (RB) as a model drug. We studied the mechanism of the drug release at different pH value. The load and release of RB were monitored by UV–Vis, and the surface topographic structure of graphene oxide was imaged by atomic force microscope (AFM). The results afford real time data and theoretical for drug load and release on graphene oxide, which may be useful for investigate the dynamic process of graphene oxide as drug carrier.

2. Materials and methods

2.1. Materials

All reagents were purchased from Sigma and were use without further purification. Graphene oxide was made by modified Hummers' method [16,17], using graphite as a starting material. GO films were made by drying GO suspension in beakers and the films were picked up by a pair of tweezers while blowing the films with humid air.

2.2. Characterizations

AFM imaging was carried out on thin GO films on silicon wafers by using a Nanoscope IIIa microscope in tapping mode. The films were first immersed in 400 mg/L RB solution for 20 h, and then were rinsed by immersing the wafer into doubly distilled water for 10 min and then by water flow for 2 min. FTIR characterizations were performed on a Nicolet 6700 (THERMO) spectrometer. RB powder, GO films, and GO films after RB loading were used to study the bond stretch in these materials, reflecting the load of RB on GO. UV–Vis was performed on a Lambda Bio 20 spectrometer (Perkin Elmer).

2.3. Loading of RB

The loading of RB on freestanding GO films was done by immersing the GO films into RB solutions, as shown in Fig. 1. For real time observation, 1 mg/L RB solution was used since 400 mg/L was too high for the UV–Vis detection. RB solution (3 ml) was added into a cuvette, and then 0.5 mg of 500 nm thick GO film was placed on the bottom of the cuvette. Absorbance of RB at 554 nm was monitored continuously for 20 h. Ex situ measurement was done by immersing the GO film in RB solution in a beaker with very slow stirring, absorbencies of the RB solution were measured from time to time during 24 h. The samples that were used for release studies were loaded in 400 mg/L of RB solution. The loading capacity was calculated by subtracting the original amount with the final amount of RB after loading (the amount of RB after the loading process was calculated from the calibration curve in Fig. S1) and then divided by the amount of GO.

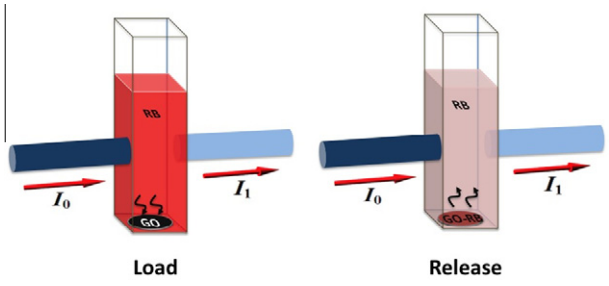

Fig. 1 – Schematic drawing of the real time monitor of drug load and release inside a cuvette.

2.4. Release of RB

To investigate the real time release of RB (Fig. 1), there were two ways to make RB loaded GO films for drug release study: (1) the films of GO were first loaded in 400 mg/L RB for 20 h to get saturated load, then the films were rinsed and dried in air. After that, 0.1 mg of the film were placed in a cuvette and different release solutions were added; (2) GO sheet suspension was mixed with RB for 20 h at a RB concentration of 400 mg/L. Then, the GO–RB hybrid was separated and rinsed by centrifuge at 4000 rpm. The separated films was then re-suspended in water and dried on an aluminum foil to get a film. The process was then proceeded as in (1) after detaching the film from the foil. Absorbance of RB at 554 nm was monitored continuously for 20 h.

3. Results and discussion

The interaction between GO and doxorubicin (DXR) can be hydrogen bonds and π–π stacking, as well as some hydrophobic force [12–15], since the –OH and –COOH groups on graphene sheet can form strong hydrogen-bonding interaction with –OH and $-NH_2$ groups in DXR. These interactions cause the high loading efficiency of DXR on GO. In our experiment, we chose rhodamine B (RB) as model drug, which also has an aromatic structure and –COOH, but without –OH and $-NH_2$ groups. Thus, there may be π–π stacking, hydrogen bonds, and electrostatic interaction since there is a nitrogen atom that could be positively charged in RB.

3.1. Loading of RB on graphene oxide

As shown in Fig. 2, RB has an obvious absorbance band around 554 nm, while GO has a characteristic band around 229 in our experiments. The interaction of these two reagents could be represented by the peak strength and position changes. We found that after the interaction, the peak of GO shifted to 231, while the peak of RB at 554 nm shifted to around 566 nm, indicating a simple π stacking between RB and GO [18], similar to that with carbon nanotube [19].

Usually, it is not easy to observe the real time loading process for nanoparticles using spectroscopy, since the dispersion of nanoparticles affect the absorption of light when it passes through the cuvette. For GO nanosheets, the same problem will appear. However, an advantage of GO sheets is

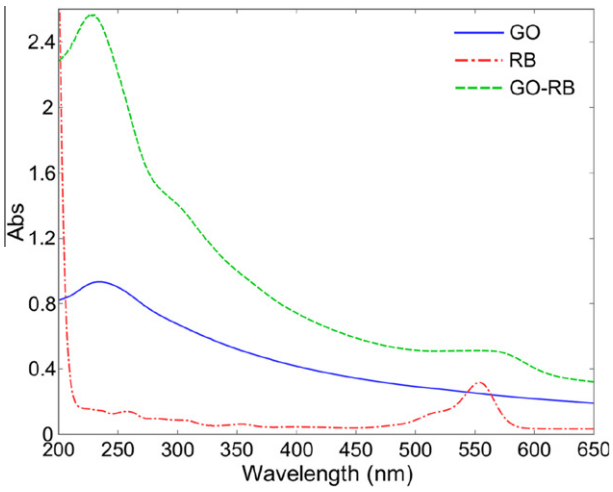

Fig. 2 – UV–Vis of graphene oxide (GO), rhodamine (RB), and GO–RB hybrid.

that they can form thin films and papers [20–23] and this is used here. Instead of using a GO suspension, we used GO films to do real time observation of loading of RB on GO by placing a GO film at the bottom of the cuvette. This placement does not block the light from passing through the RB solution.

To calibrate the set-up we compared the loading efficiency of the GO suspension and the GO films. We used two samples with same amount of GO, one was suspended in RB solution, and the other was made as GO films (about 500 nm thick) and then put into RB solution. After 20 h loading, we found that the loading efficiency of GO films were 80–90% of the capacity of the GO suspension, making the two set-ups comparable.

Fig. 2 shows the real time and non-real time observation of the loading process and almost 95% of RB in the solution was loaded on GO films by calculating the RB residue in the solution after loading process. Fig. 3 also shows a photograph of RB before and after the loading process with a clear change of color, indicating high efficiency of the loading of RB on

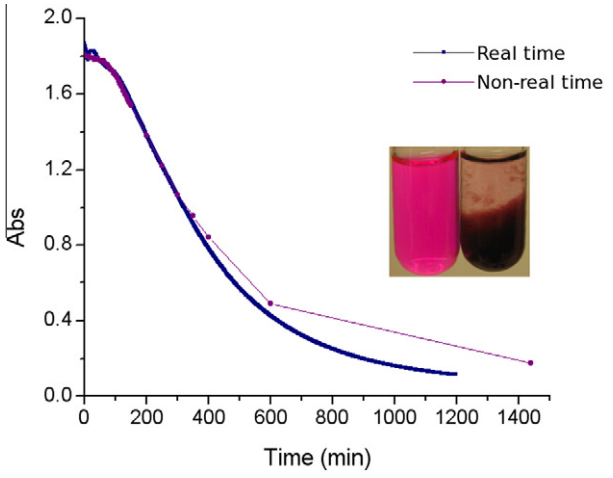

Fig. 3 – Real time and non-real time loading curves. The inserted image shows the RB solution and GO–RB hybrid suspension.

GO. The UV–Vis curve of RB solution before and after loading is given in Fig. 4C, showing the absorbance change of RB.

Fig. 4A shows a schematic drawing of the binding of RB to GO sheet. To further investigate the interaction of GO with RB, we did FT-IR experiments. Fig. 4B shows the FT-IR of RB, GO and GO–RB hybrid. In the FTIR of GO–RB, the existence of –OH (~3400 cm^{-1}), C=O (1716 cm^{-1}) and C=C (1617 cm^{-1}) indicated the functional groups in GO [24,25], and the existence of band at 1586 and 1331 cm^{-1} indicated the deposition of RB on GO films [26].

To observe the surface topographic structure of GO after the load of RB, we first deposited a thin GO layer (film thickness was about 2 nm) on a silicon wafer and then put it into the RB solution for 20 h.

AFM imaging, see Fig. 5, show that after the deposition process, the GO film was coated with extra layer RB. At higher magnification the porous structure of the RB film was revealed. From the AFM imaging the average thickness of RB layer on GO was measured to 1–3 nm. It is not to easy to say that there is some specific binding sites of RB on the GO, but the porous RB layer seems very even.

There are several mechanisms of binding RB to other molecules or materials, which are pH dependent [27]. At pH value less than 5, protonated RB will easily bind to GO [27]. In our experiment, the loading process was in a 400 mg/L RB solution, with a measured pH of 3.35. This low pH value aided the binding process of RB to GO, since the GO sheets are more hydrophobic [28] and can interact with RB through hydrophobic force at this low pH value. Moreover, the –COOH group can form hydrogen bond with GO at pH 3.35, since the *pKa* value of RB is 4.2 [29]. Electrostatic interaction might be another force for RB loading, but since the *pKa* distribution of GO is higher than 3.35 [30], the GO sheets show less negative charge, resulting in less electrostatic interaction since RB is positively charged at this pH value. To increase binding of RB on GO our loading process was performed at pH 3.35 and a 0.5 mg/mg loading capacity of RB to GO was achieved with an initial RB loading concentration of 400 mg/L. Compared with DXR [14], the loading capacity of RB is lower. There are two reasons for this. Firstly the structure of DXR is more flat than RB, which make the π–π stack stronger; secondly DXR contains more –OH group, which can form more hydrogen bonds with GO.

3.2. *Release of RB from GO*

The same problem of the blocking of light in a GO solution, as mentioned above, inhibits real time observation. However, we can use a slightly modified version of the method that we described above for real time monitoring the loading of RB on GO. We dried the loaded GO film and let the film float on the solvent which were used to investigate the release process, making it easy to monitor it in real time.

Fig. 6 shows the real time release of RB in doubly distilled water and phosphate buffer solution (PBS) at pH 4.5 and pH 7.4. Different release behaviors of RB were observed in these three solutions. In aqueous, RB released slowly and achieved a stable level after 20 h. In pH 4.5 PBS, the release speed is higher than in doubly distilled water. But in pH 7.4 PBS, RB quickly released from GO and achieves the stable level within 1.5 h.

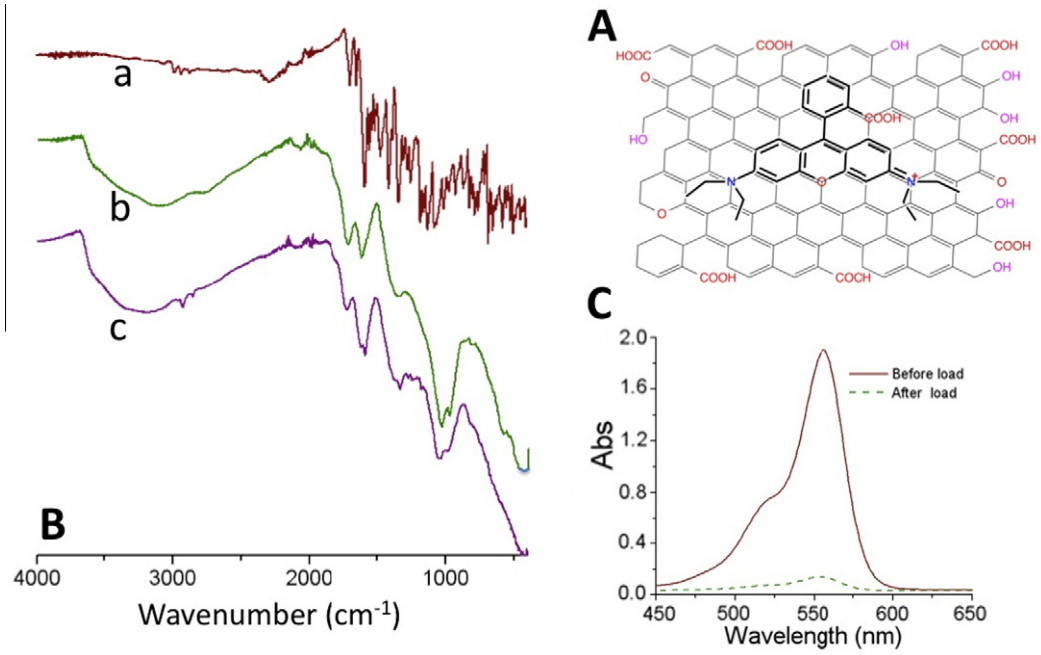

Fig. 4 – (A) Schematic drawing of the binding of rhodamine B to graphene oxide. (B) FTIR spectra of (a) rhodamine B, (b) graphene oxide and (c) rhodamine B loaded graphene oxide. (C) The UV–Vis of rhodamine B before and after loading, showing that more than 90% of rhodamine B has been loaded on graphene oxide.

The accumulative release of RB in PBS after 20 h were about 90% at pH 7.4 and 75% at pH 4.5 (after 40 h the release was 90% for pH 4.5 PBS, as shown in Supporting information as Fig. S2), but the value was less than 20% for doubly distilled water.

According to the drug release equation for a thin slab [31,32], the drug release can be empirically expressed as

$$\frac{M_i}{M_\infty} = kt^n, \quad (1)$$

where M_i/M_∞ is the fraction of drug released at time t, and where k and n are constants. For a film, $n > 0.5$ indicates anomalous or non-Fickian transport, $n = 1$ indicates case II (relaxation-controlled) transport, and $n \leqslant 0.5$ implies Fickian diffusion [33]. We can fit this equation to our experimental data to reveal the constant n. For drug release in pH 7.4 PBS, $n = 1$, which is a relaxation controlled or Case II transport process [34]. For pH 4.5 PBS the diffusion is non-Fickian with $n = 0.635$ and also for water where the fitted value was found to be $n = 0.631$.

The sample is a stack of RB coated GO sheets and the diffusion of RB is related to the transport between the sheets in the stack. However, the GO–RB interaction is of major importance, since the samples were prepared in such a way that only a thin layer of RB was deposited on the GO sheets. The amount of RB between the layers is thus small compared to the amount deposited on the GO sheets. Therefore the type of solvents and the ionic strengths are important to consider in the discussion of the release process.

First, we discussed the differences of release in PBS buffer at different pH. Based on the structure of RB and GO, there could be hydrogen bonds, electrostatic interaction, and hydrophobic interaction (including π–π stack) between these two molecules, which all are pH dependent. At low pH value GO sheets are more hydrophobic leading to stronger interaction with RB than at higher pH [28]. Hydrogen bond, as described above in Section 3.1, aids deposition of RB on GO, since the pH value is lower than the *pKa* value (4.2), when the –COOH group is not deprotonized. The –COOH can interact with both –OH and –COOH groups on GO at low pH values. But when the pH value increases, that is when the –COOH groups are deprotonized, the capability of hydrogen bond formation between the –COOH groups get weaker. Although the –OH group is more active in forming hydrogen bond, the –COOH group of RB is less active, making the total probability lower of hydrogen bond formation at high pH. Thus, at pH 4.5, the possibility of hydrogen bond formation is stronger than at pH 7.4. Electrostatic interaction was not considered in the discussion above on loading of RB, but it might be of importance in the release of RB. At the loading pH value of 3.35, GO sheets are less negatively charged, thus the electrostatic interaction between these two molecules is weak. But at the release pH values of PBS at 4.5 and 7.4, the GO sheets are more negatively charged, causing electrostatic interaction between –COOH of GO and N^+ of RB. Ramette and Sandell described that RB commonly contains a negatively charged –COOH group and a positively charged N atom in polar solvents like water [35]. Thus, the electrostatic interaction of GO and RB is more complicated at different pH. At low pH value, GO is less negatively charged, thus, the electrostatic interaction between GO and RB is weak. While at high pH value, GO is more negatively charged; RB is also more negatively charged. Thus, although a more negatively charged GO has a more electrostatic affinity to the N^+ atom, the electrostatic interaction might also be weak, since the total RB charge is negative, leading to an electrostatic repulsion between GO and RB. Thus, from the information available in our experiments it is hard to tell

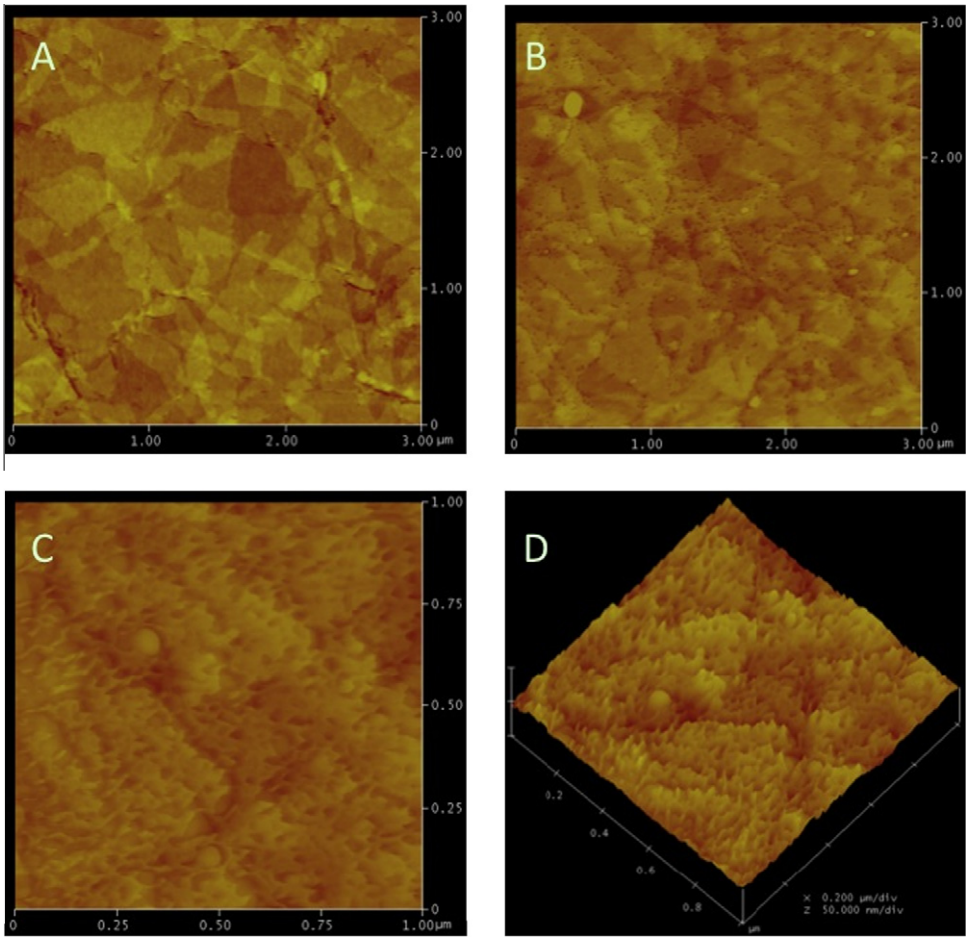

Fig. 5 – AFM of graphene oxide (A) (3 × 3 μm) and rhodamine B loaded graphene oxide (B) (3 × 3 μm). (C and D) Show the AFM of (B) at higher magnification (1 × 1 μm) and in 3D model (the height scale is 50 nm/division).

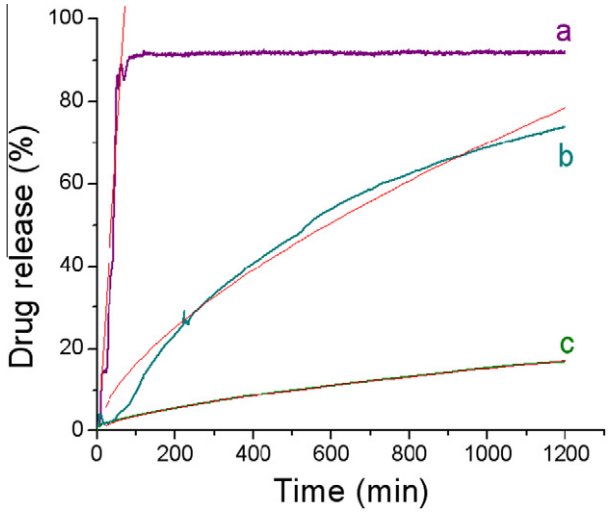

Fig. 6 – Real time cumulative release of (a) RB in pH 7.4 (b), RB in pH 4.5 PBS, and (c) RB in water solution. The red lines are from the model according to Eq. (1).

how the electrostatic force works exactly at different pH, and more studies are needed.

Besides the interaction between GO and RB, the solubility of RB and different pH value might also influence the drug release behavior. Ramette and Sandell pointed out the molar solubility of RB increase with increasing acid concentration [35]. Thus, at low pH, the RB might be release faster in our experiment, but such influence of the solubility was not directly studied here. It might give some contribution, but the influence of the solubility should be much less than the interactions discussed above.

In summary, the hydrophobic force (including π–π stack) and hydrogen bond between GO and RB influenced the drug release of RB at different pH values. Electrostatic interaction might also play a role in the release process, but since RB contains both positive and negative charged groups in polar solvents like water [35], additional work is needed to clarify this.

However, we cannot use this explanation for water because, as illustrated in Fig. 5, the cumulative release of both pH 7.4 and pH 4.5 PBS was both higher than water. Instead, this may due to the ionic strength of the solutions as this will decreased the cumulative release of drugs [34]. Ionic strength is related to the strength of electrostatic interaction between RB and GO, and the higher strength in PBS will reduce the electrostatic interaction between RB and GO.

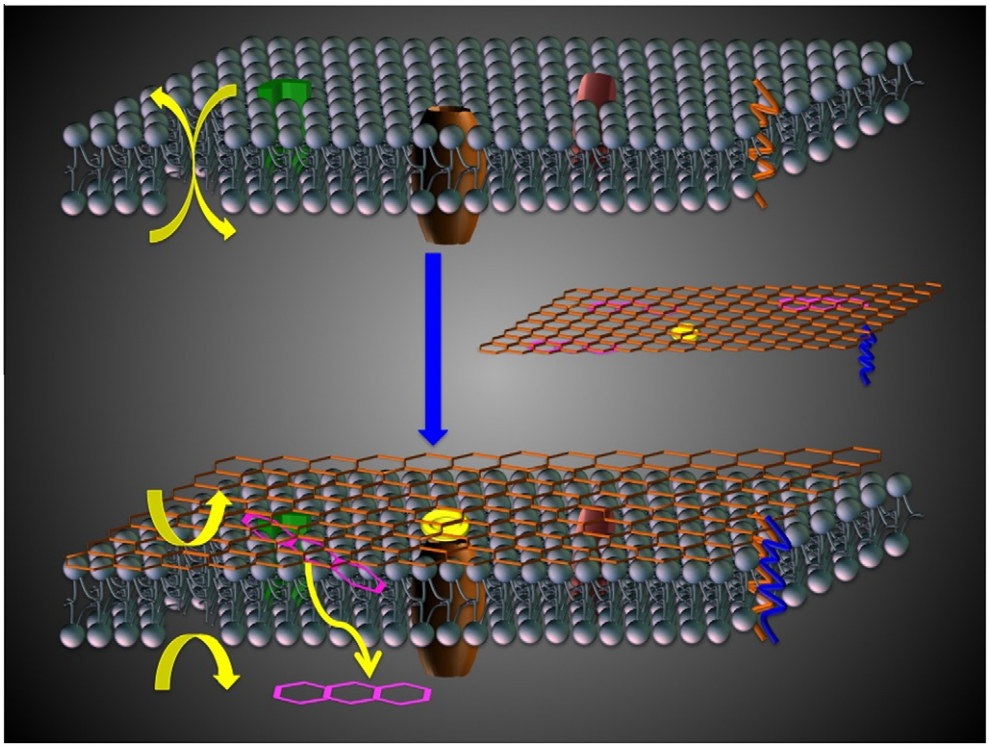

Fig. 7 – Potential application hypothesis of GO as both drug carrier and blocker for cell communication.

3.3. *Potential application hypothesis*

There are several investigations about the application of GO in drug delivery [12–15] including experiments at the cell level [13,15] showing that GO can serve as a versatile drug carrier due to the structure. The group of Dai investigated the modification of GO sheets with polyethylene glycol (PEG) conjugated with rituxan, which is a B-cell antibody, showing the recognition of cells to modified GO [13].

Based on this, we can ask the question, whether the GO sheets can be used as a blocking material to cover the cell membranes of mutated cells. As shown in Fig. 7, a cell has both intra- and extra-cellular flux, and this cell communication is of outmost importance for the cell. One may develop a scheme to kill mutated cells by blocking this cell membrane communication. For example, modified GO sheets, with both drugs and substrates for cell membrane proteins, may be recognized by the cell membrane proteins and then tightly attached to the cell, accompanying with delivery of drugs to the cell. This tight coat may then block or reduce the matter and energy exchange between the two sides of cell membrane, causing the death or lowering of the activities of the mutated cells. One should point out that the GO sheet here is hypothesized to be individually dispersed, but since the graphene layer now can be synthesized with a very large area [36], in vitro experiment on single cells might be achieved.

However, based on the GO films described in this paper, it is not easy to test the single cell hypothesis, but something similar might be possible. The GO films here can be made as a patch, which can then be attached on wounded skin, or organ membrane. For example, a small GO patch loaded with drugs can be placed on a wounded gastric mucosal. With this patch, the drugs can be delivered to the wounded place. Moreover, the patch can protect the mucosal from potential external infection.

Compared with other nanoparticles that are used as drug carrier, the 2D structure of GO adds this new possibility to tightly coated and block cell communications of the cells, and may be used as potential patch for the treatment of wounded organ. These features might lead to a new strategy for medical applications.

4. Conclusions

In summary, we have studied graphene oxide (GO) sheets as drug carrier by using an in vitro real time monitoring method. Rhodamine B (RB) was used as model of a drug. Real time experimental results indicated that RB can be loaded on GO with a capacity of 0.5 mg/mg, which is lower than reported DXR and was probably due to less hydrogen bonding sites and the less flat molecular structure of RB. The drug release of RB was pH sensitive as observed at pH 7.4 and pH 4.5 PBS solutions. Higher pH values lead to weaker hydrophobic interaction and hydrogen bonds, and thus higher release rate. Electrostatic interaction might aid the release of the RB, but the mechanism of how it works at different pH needed more studies. Moreover, ionic strength also influenced the release of RB, as shown from the different release rates between PBS solutions and double distilled water. These results indicated an anomalous diffusion process at pH 4.5 and in water and a case II transport process at pH 7.4. The results also indicated a high loading capacity of RB on GO and a high cumulative release in phosphate buffers. These results point to potential application of GO in drug delivery and we also dis-

cussed the possibility to use the GO for blocking matter exchange of mutated cells due to its 2D structure, as well as the GO films for protecting wounded skin as patches. The real time method described here allows real time determination of drug release from GO and might thus complement other tools used for studies of drug release systems. For example, compared with common dialysis analysis, the in vitro determination shows real time data of drug load and release. This real time method might also be of importance in other biomedical investigations.

Acknowledgement

We thank the Sundsvall Community for financial support.

Appendix A. Supplementary data

Supplementary data associated with this article can be found, in the online version, at doi:10.1016/j.carbon.2010.11.026.

REFERENCES

[1] Chi FL, Guo YN, Liu J, Liu YL, Huo QS. Size-tunalbe and functional core-sheel structured silica nanoparticles for drug release. J Phys Chem C 2010;114:2519–23.
[2] Ferrari M. Cancer nanotechnology:opportunities and challenges. Nat Rev Cancer 2005;5:161–71.
[3] Suh WH, Suh Y-H, Stucky GD. Multifunctional nanosystems at the interface of physical and life sciences. Nano Today 2009;4:27–36.
[4] Zhang RY, Wang XM, Wu CH, Song M, Li JY, Lv G, et al. Synergistic enhancement effect of magnetic nanoparticles on anticancer drug accumulation in cancer cells. Nanotechnology 2006;17:3622–6.
[5] Brigger I, Dubernet C, Couvreur P. Nanoparticles in cancer therapy and diagnosis. Adv Drug Deliv Rev 2002;54:631–51.
[6] LaVan DA, McGuire T, Langer R. Small-scale systems fro in vivo drug delivery. Nat Biotech 2003;21:1184–91.
[7] Ghosh P, Han G, De M, Kim CK, Rotello VM. Gold nanoparticles in delivery applications. Adv Drug Deliv Rev 2008;60:1307–15.
[8] Panyam J, Labhasetwar V. Biodegradable nanoparticles for drug and gene delivery to cells and tissue. Adv Drug Deliv Rev 2002;55:329–47.
[9] Cho K, Wang X, Nie SM, Chen Z, Shi DM. Therapeutic nanoparticles fro drug delivery in cancer. Clin Cancer Res 2008;14:1310–6.
[10] Qiu LY, Bae YH. Polymer architecture and drug delivery. Pharm Res 2006;23:1–30.
[11] Jain TK, Morales MA, Sahoo SK, Leslie-Pelecky DL, Labhasetwar V. Iron oxide nanoparticles for sustained delivery of anticancer agents. Mol Pharm 2005;2:194–205.
[12] Liu Z, Robinson JT, Sun XM, Dai HJ. PEGylated nanographene oxide for delivery of water-insoluble cancer drugs. J Am Chem Soc 2008;130:10876–7.
[13] Sun XM, Liu Z, Welsher K, Robinson JT, Goodwin A, Zaric S, et al. Nano-graphene oxide for cellular imaging and drug delivery. Nano Res 2008;1:203–12.
[14] Yang XY, Zhang XY, Liu ZF, Ma YF, Huang Y, Chen YS. High-efficiency loading and controlled release of doxorubicin hydrochloride on graphene oxide. J Phys Chem C 2008;112:17554–8.
[15] Zhang LM, Xia JG, Zhao QH, Liu LW, Zhang ZJ. Functional graphene oxide as a naocarrier for controlled loading and targeted delivery of mixed anticancer drugs. Small 2009;6:537–44.
[16] Hummers WS, Offeman RE. Preparation of graphitic oxide. J Am Chem Soc 1958;80:1339.
[17] Hirata M, Gotou T, Horiuchi S, Fujiwara M, Ohba M. Thin-film particles of graphite oxide 1:high-yield synthesis and flexibility of the particles. Carbon 2004;42:2929–37.
[18] Fletcher BL, McKnight TE, Melechko AV, Simpson ML, Doktycz MJ. Biochemical functionalization of vertically aligned carbon nanofibres. Nanotechnology 2006;17:2032–9.
[19] Liu Z, Sun XM, Nakayama-Ratchford N, Dai HJ. Supramolecular chemistry on water-soluble carbon nanotubes for drug loading and delivery. ACS Nano 2007;1:50–6.
[20] Dikin DA, Stankovich S, Zimney EJ, Piner RD, Dommett GHB, Evmenenko G, et al. Preparation and characterization of graphene oxide paper. Nature 2007;448:457–60.
[21] Eda G, Fanchini G, Chhowalla M. Large-area ultrathin films of reduced graphene oxide as a transparent and flexible electronic material. Nat Nanotech 2008;3:270–4.
[22] Park S, Lee K-S, Bozoklu G, Cai WW, Nguyen ST, Ruoff RS. Graphene oxide papers modified by divalent ions-enhancing mechanical properties via chemical cross-linking. ACS Nano 2008;2:572–8.
[23] Cote LJ, Kim F, Huang JX. Langmuir-blodgett assembly of graphite oxide single layers. J Am Chem Soc 2008;131:1043–9.
[24] Hontoria-Lucas C, Lopez-Peinado AJ, Lopez-Gozalez JDD, Rojas-Cervantes ML, Martin-Aranda RM. Sduty of oxygen-containing groups in a series of graphite oxides: physical and chemical characterization. Carbon 1995;33:1585–92.
[25] Szabo T, Berkesi O, Dekany I. DRIFT study of deuterium-exchanged graphite oxide. Carbon 2005;43:3186–9.
[26] Chouket A, Elhouichet H, Oueslati M, Koyama H, Gelloz B, Koshida N. Energy transfer in porous-silicon/laser-dye composite evidenced by polarization memory of photoluminescence. Appl Phys Lett 2007;91:211902.
[27] Moreno-Villoslada I, Jofré M, Miranda V, González R, Sotelo T, Hess S, et al. PH dependence of the interaction between rhodamine B and the water-soluble poly(sodium 4-styrenesulfonate). J Phys Chem B 2006;110:11809–12.
[28] Kim A, Cote LJ, Yuan W, Shull KR, Huang JX. Graphene oxide sheets at interface. J Am Chem Soc 2010;132:8180–6.
[29] Hii S-L, Yong S-Y, Wong C-L. Removal of rhodamine B from aqueous solution by sorption on Turbinaria conoides (Phaeophyta). J Appl Phycol 2009;21:625–31.
[30] Petit C, Seredych M, Bandosz TJ. Revisiting the chemistry of graphite oxides and its effect on ammonia adsorption. J Mater Chem 2009;19:9176–85.
[31] Langer RS. Peppas, NA, Present and future applications of biomaterials in controlled drug delivery systems. Biomaterials 1981;2:201–14.
[32] Vrentas JS, Jarzebski CM. Duda JL A deborah number for diffusion in polymer-solvent system. AIChE J 1975;21:894–901.
[33] Kim B, Flamme KL, Peppas NA. Dynamic swelling behavior of pH-sensitive anionic hydrogels used for protein delivery. J Appl Poly Sci 2003;89:1606–13.
[34] Shu ZX. Zhu KJ Controlled drug release properties of ionically cross-linked chitosan beads:the influence of anion structure. Inter J Pharm 2002;233:217–25.
[35] Ramette RW, Sandell EB. Rhodamine B equilibria. J Am Chem Soc 1956;78:4782–8.
[36] Lee Y, Bae S, Jang H, Jang S, Zhu S-E, Sim SH, et al. Wafer-scale synthesis and transfer of graphene films. Nano Lett 2010;10:490–3.